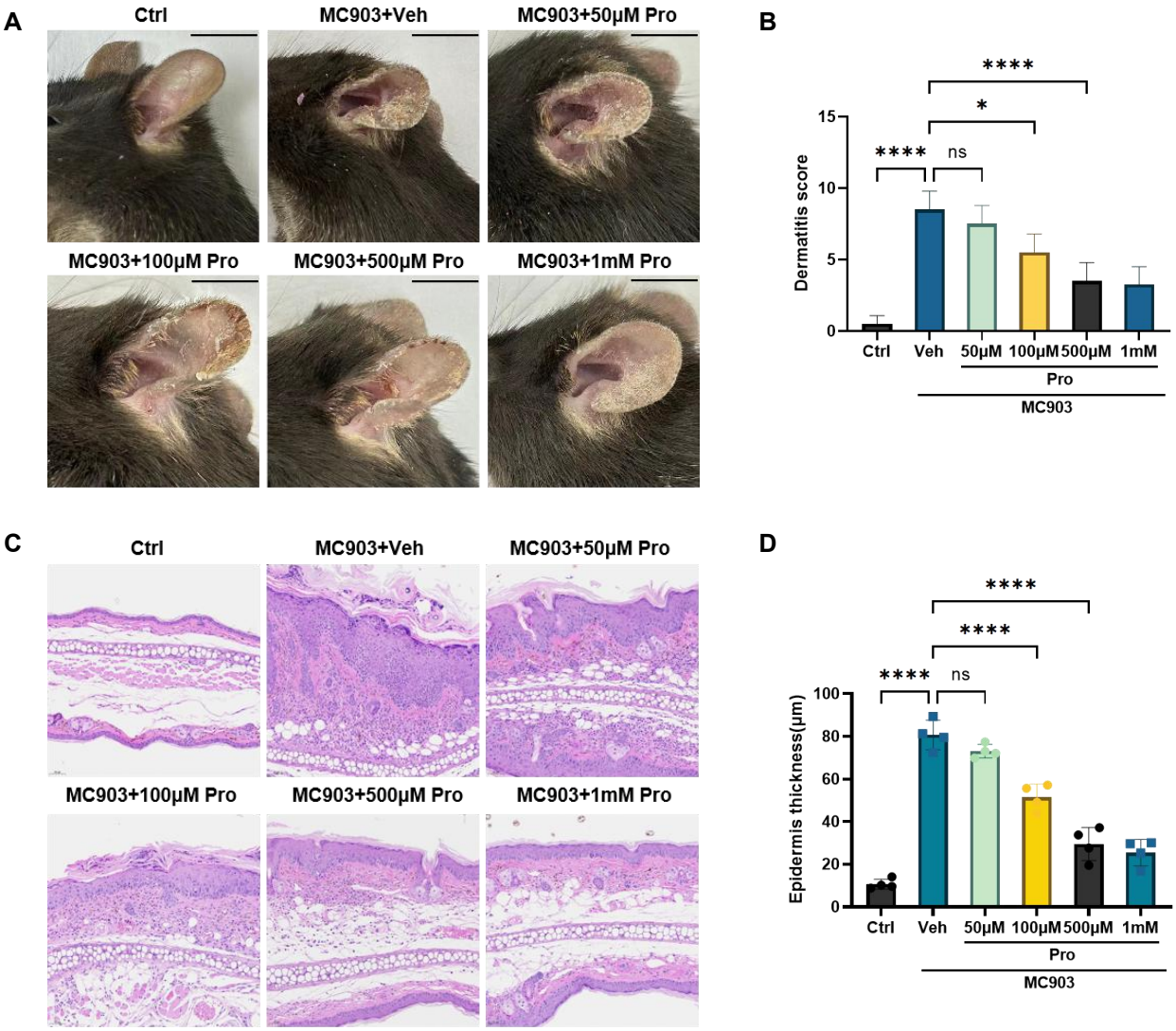

Figure S1. Propionate dose-dependently alleviates skin inflammation. Related to Figure 1.
(A) Representative images of skin lesions in MC903 mice treated with a concentration gradient of propionate (Scale bar = 1 cm).
(B) Statistical result for dermatitis scores of each group.
(C) H&E staining of mouse ear tissues (Scale bar = 50 μm).
(D) Statistical result for epidermis thickness of each group.
Data are represented as mean ± SEM, n = 4 mice/group, one-way ANOVA followed by Tukey honest significant difference post-hoc test for multiple comparisons, ns=no significance, *p<0.05, **p<0.01 and ****p<0.0001. Veh, vehicle control; Pro, propionate; Ctrl, control.

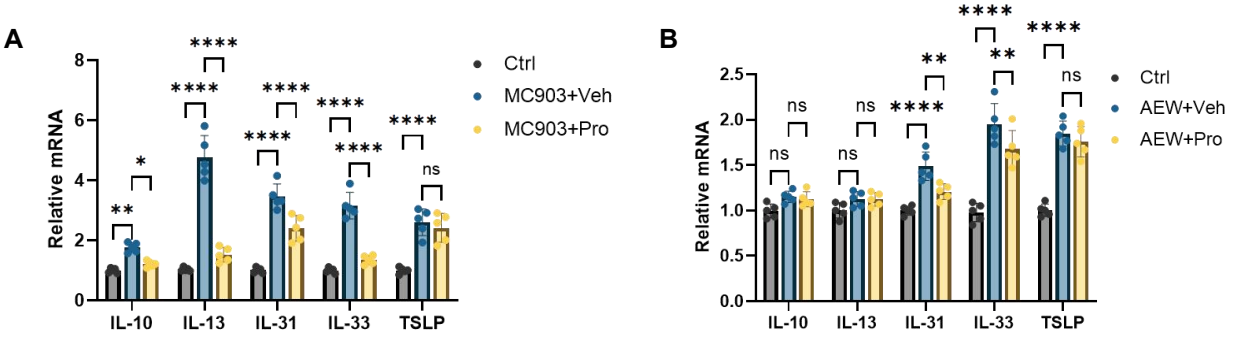

Figure S2. Propionate modulates inflammatory cytokines. Related to Figure 2.
(A) Relative mRNA levels of inflammatory cytokines in MC903 mouse skin lesions from each group.
(B) Relative mRNA expression of various cytokines in AEW mice.
Data are represented as mean ± SEM, n = 5 mice/group, one-way ANOVA followed by Tukey honest significant difference post-hoc test for multiple comparisons, ns=no significance, *p<0.05, **p<0.01 and ****p<0.0001. AEW, acetone-ether-water; Veh, vehicle control; Pro, propionate; Ctrl, control.

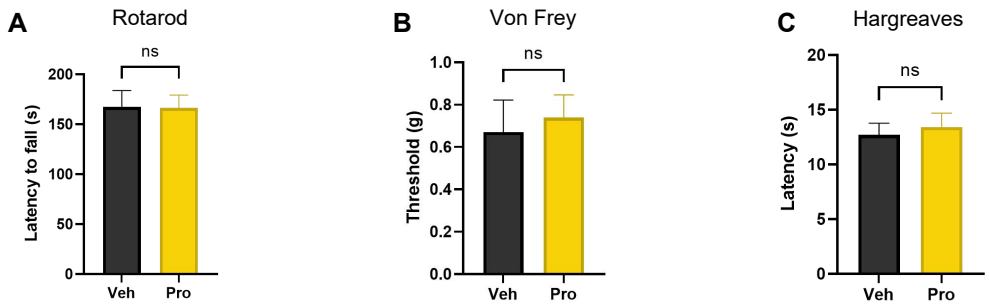

Figure S3. Propionate is not involved in nociception. Related to Figure 2.
(A) Latency to fall assessed by rotarod in mice treated with propionate or vehicle control.
(B) Paw withdrawal threshold in response to mechanical stimuli after intraplantar injections of 4 mM propionate or 10 µl vehicle in mice.
(C) Paw withdrawal threshold in response to thermal stimuli.
Data are represented as mean ± SEM, n = 5-6 mice/group, two-tailed unpaired Student's t-test, ns=no significance, *p<0.05, **p<0.01 and ****p<0.0001. Veh, vehicle control; Pro, propionate.

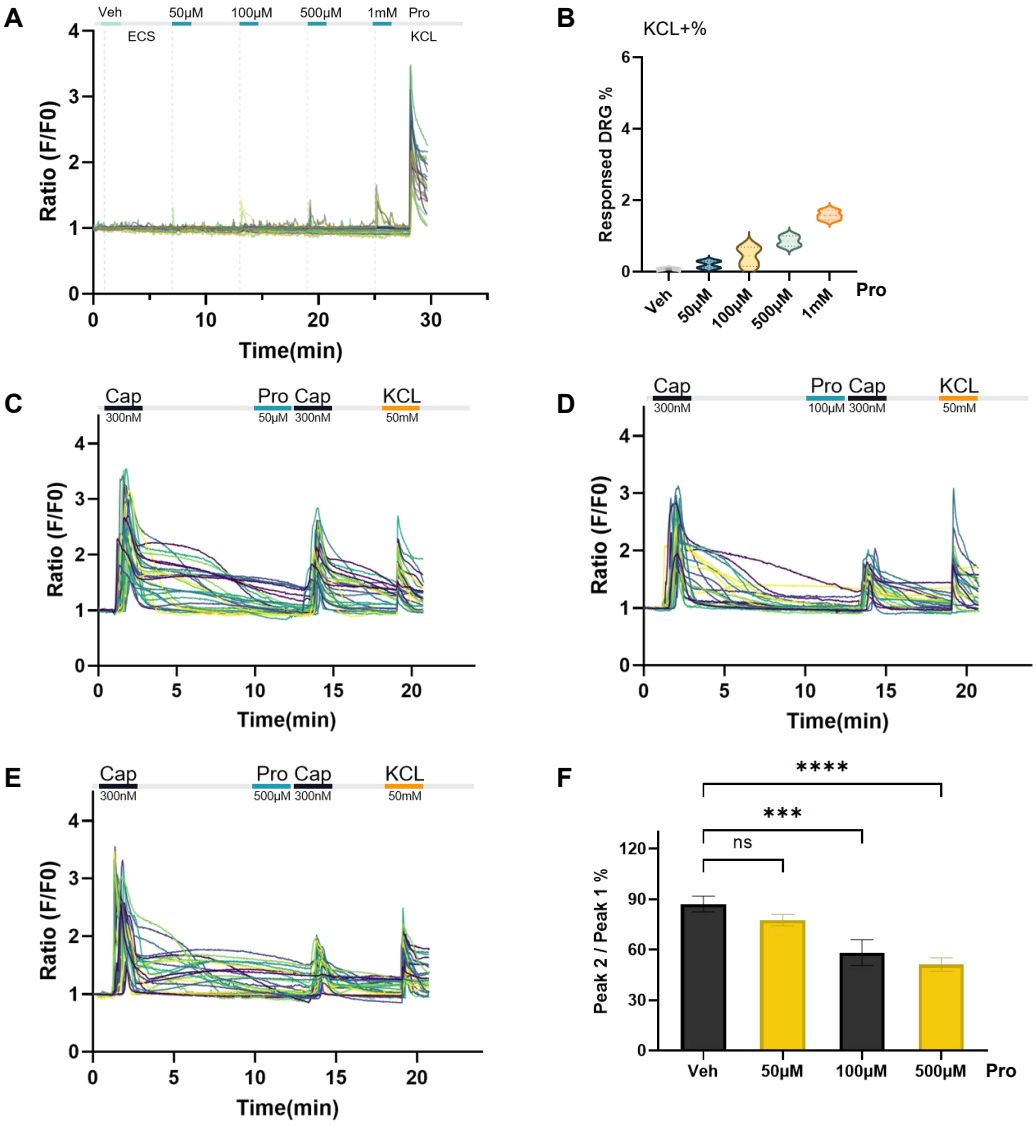

Figure S4. Propionate reduces calcium responses of DRG neurons to capsaicin. Related to Figure 3.

(A) Calcium imaging trace of DRG neurons exposed to vehicle and increasing doses of propionate.
(B) Quantification of total KCl-responsive neurons responding to increasing doses of propionate.
(C-E) Representative calcium imaging trace of mouse DRG neurons responding to capsaicin after treatment with a concentration gradient of propionate.
(F) Peak2/Peak1 ratio denoting calcium influx evoked by capsaicin in the presence of propionate.
N > 100 DRG neurons from 5-10 WT mice. Data are represented as mean ± SEM, one-way ANOVA followed by Tukey honest significant difference post-hoc test for multiple comparisons, ns=no significance, *p<0.05, ***p<0.001 and ****p<0.0001. Cap,capsaicin; ECS, extracellular solution; Veh, vehicle control; Pro, propionate.

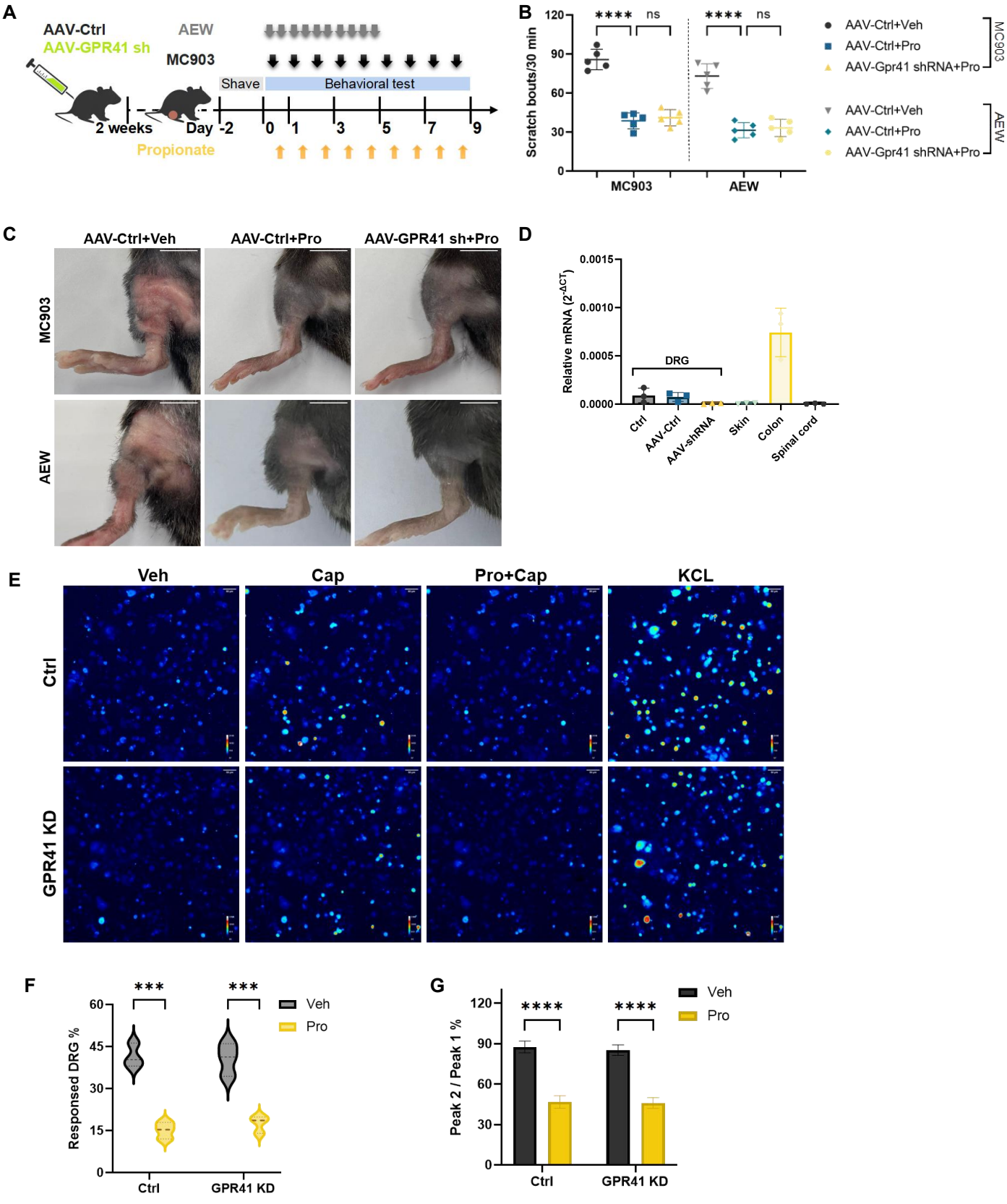
A
AAV-Ctrl
AAV-GPR41 sh
AEW
MC903
Shave
Behavioral test
2 weeks
Day -2
0
1
3
5
7
9
Propionate
B
Scratch bouts/30 min
****
ns
MC903
AEW
AAV-Ctrl+Veh
AAV-Ctrl+Pro
AAV-Gpr41 shRNA+Pro
C
AAV-Ctrl+Veh
AAV-Ctrl+Pro
AAV-GPR41 sh+Pro
MC903
AEW
D
Relative mRNA (2-ΔCT)
DRG
Ctrl
AAV-Ctrl
AAV-shRNA
Skin
Colon
Spinal cord
E
Veh
Cap
Pro+Cap
KCL
Ctrl
GPR41 KD
F
***
Responsed DRG %
Veh
Pro
Ctrl
GPR41 KD
G
****
Peak 2 / Peak 1 %
Veh
Pro
Ctrl
GPR41 KD

Figure S5. Propionate protects against itch independent of GPR41. Related to Figure 4.
(A) Schematic protocol of GPR41 knockdown and induction of AEW/MC903 model.
(B) Numbers of spontaneous scratching bouts among different groups.
(C) Representative images of hind paw skin lesions (Scale bar = 1 cm).
(D) Relative GPR41 gene expression in mice tissues.
(E) Calcium imaging of DRG neurons from Ctrl or GPR41 knockdown mice responding to capsaicin.
(F) Changes in percentage of capsaicin-responsive DRG neurons with or without propionate among each group.
(G) Propionate-affected magnitude of calcium influx in DRG neurons from Ctrl and GPR41 knockdown group.
Data are represented as mean ± SEM, n = 5-6 mice/group, one-way ANOVA followed by Fisher's least significant difference post hoc correction for multiple comparisons, ns=no significance, *p<0.05, **p<0.01 and ****p<0.0001. AEW, acetone-ether-water; Veh, vehicle control; Pro, propionate; Ctrl, control; Cap,capsaicin; KD, knockdown.

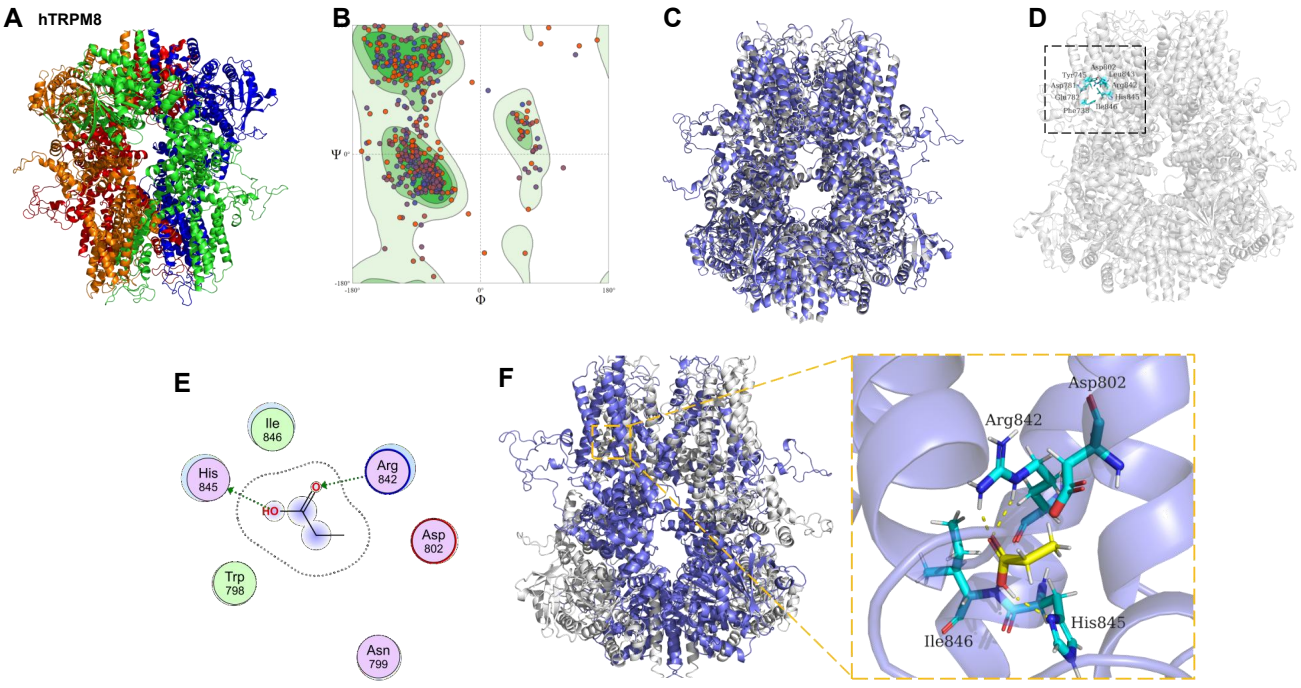

Figure S6. Molecular docking of propionate and hTRPM8. Related to Figure 5.
(A) Homology model of TRPM8.
(B) Ramachandran plot for TRPM8. Dark blue dots represent the residues in favored regions; orange dots represent the residues in allowed regions.
(C) Structural analysis of TRPM8 modeling results.
(D) Binding site of propionate in TRPM8.
(E) 2D binding mode of propionate and TRPM8.
(F) 3D binding mode of propionate and TRPM8. The hydrogen bonds are depicted as yellow dashed lines. The surrounding residues in the binding pocket are colored in cyan.

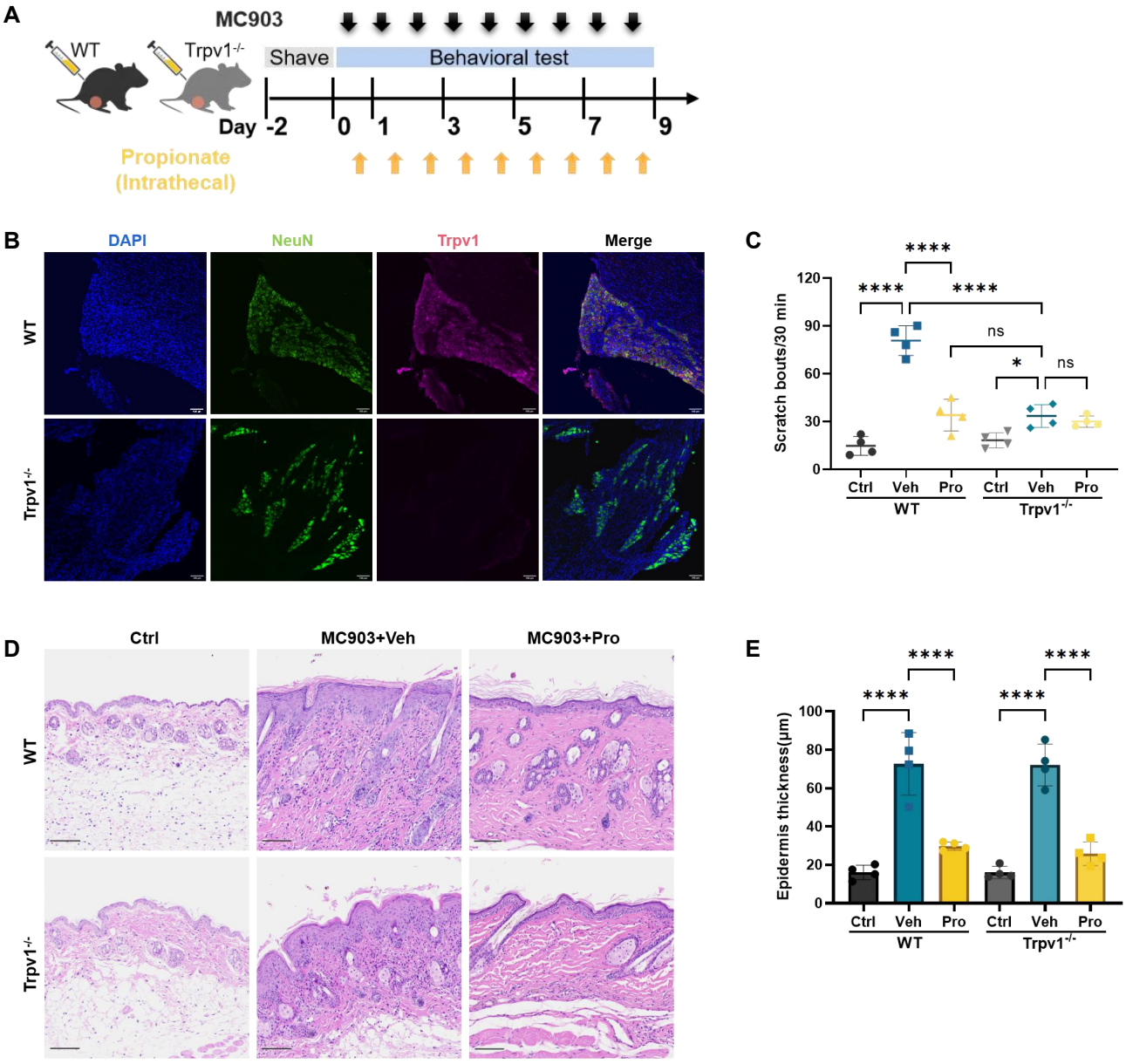

Figure S7. Genetic ablation of Trpv1 attenuates MC903-induced itch. Related to Figure 5.
(A) Schematic protocol of induction of MC903 model in WT and *Trpv1*$^{-/-}$ mice.
(B) Representative immunofluorescent images of trigeminal ganglia (TG) stained with DAPI (blue), NeuN (green) and Trpv1 (pink) (Scale bar = 100 μm).
(C) Numbers of spontaneous scratching bouts among different groups.
(D-E) Histopathology of skin tissues. Results of H&E staining are shown in (D) (Scale bar = 100 μm), and statistical result for epidermis thickness of each group is shown in (E).
Data are represented as mean ± SEM, n = 4 mice/group, one-way ANOVA followed by Fisher's least significant difference post hoc correction for multiple comparisons, ns=no significance, *p<0.05, **p<0.01 and ****p<0.0001. AEW, acetone-ether-water; Veh, vehicle control; Pro, propionate; Ctrl, control.

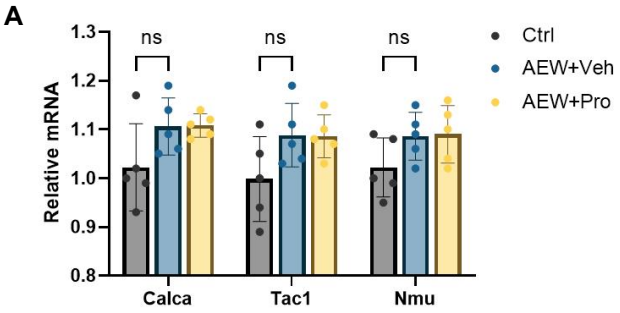

Figure S8. Propionate regulates inflammatory cytokines. Related to Figure 6.
(A) Relative mRNA levels of neuropeptides in AEW mouse skin lesions from each group.
Data are represented as mean ± SEM, n = 5 mice/group, one-way ANOVA followed by Tukey honest significant difference post-hoc test for multiple comparisons, ns=no significance. AEW, acetone-ether-water; Veh, vehicle control; Pro, propionate; Ctrl, control.